Radiology: Imaging Cancer

REVIEW

# Infrared Fluorescence-guided Surgery for Tumor and Metastatic Lymph Node Detection in Head and Neck Cancer

*Haley W. White, BA • Abdullah Bin Naveed, MBBS • Benjamin R. Campbell, MD • Yu-Jin Lee, MD • Fred M. Baik, MD • Michael Topf, MD • Eben L. Rosenthal, MD • Marisa E. Hom, PhD*

From the University of Michigan School of Medicine, Ann Arbor, Mich (H.W.W.); Department of Otolaryngology-Head and Neck Surgery, Vanderbilt University Medical Center, 2220 Pierce Ave, PRB 754, Nashville, TN 37232 (A.B.N., B.R.C., M.T., E.L.R., M.E.H.); and Department of Otolaryngology-Head and Neck Surgery, Stanford University School of Medicine, Stanford, Calif (Y.J.L., F.M.B.). Received October 9, 2023; revision requested November 15; revision received May 13, 2024; accepted May 24. **Address correspondence to** M.E.H. (email: *marisa.e.hom@vumc.org*).

Authors declared no funding for this work.

Conflicts of interest are listed at the end of this article.

*Radiology: Imaging Cancer* 2024; 6(4):e230178 • https://doi.org/10.1148/rycan.230178 • Content codes: HN IR OI

In patients with head and neck cancer (HNC), surgical removal of cancerous tissue presents the best overall survival rate. However, failure to obtain negative margins during resection has remained a steady concern over the past 3 decades. The need for improved tumor removal and margin assessment presents an ongoing concern for the field. While near-infrared agents have long been used in imaging, investigation of these agents for use in HNC imaging has dramatically expanded in the past decade. Targeted tracers for use in primary and metastatic lymph node detection are of particular interest, with panitumumab-IRDye800 as a major candidate in current studies. This review aims to provide an overview of intraoperative near-infrared fluorescence-guided surgery techniques used in the clinical detection of malignant tissue and sentinel lymph nodes in HNC, highlighting current applications, limitations, and future directions for use of this technology within the field.



In patients with head and neck cancer (HNC), surgical removal of cancerous tissue presents the best overall survival rate compared with treatment with radiation therapy or chemotherapy (1). Failure to obtain complete surgical resection of malignant tissue with negative margins is associated with local-regional recurrence and poor patient survival (2–6). Complete removal of cancerous tissue and detection of metastatic lymph nodes (LNs) must be carefully balanced with preservation of healthy tissue because of the poor functional and cosmetic quality of life outcomes often associated with oncologic resection of HNCs (7). Correct identification of tumor tissue thus remains paramount; however, rates of positive margins in solid tumor HNCs have remained steady at roughly 13% (15 411 of 120 826) over the past few decades, underscoring the need for improved tumor identification techniques within the field (8,9).

Current methods for tumor identification in HNC rely on preoperative imaging, knowledge of anatomic landmarks, and both intraoperative visualization and physical palpation by the surgeon. Palpation and white light visualization are often insufficient methods of determining location and extent of malignant tissue, particularly when the microscopic margins blur with complex surrounding tissue of the head and neck (10,11). Moreover, while CT, MRI, SPECT, and PET are used extensively for noninvasive oncologic imaging, their application is not consistently available in the operating room due to the size of equipment and cost of application (12,13). Use of intraoperative US for determination of tumor thickness and depth in HNC has been investigated with some success; however, the technique is not currently widely used (14,15). The only broadly accepted form of intraoperative margin assessment is frozen-section analysis (FSA), which allows for histologic analysis of tissue samples to identify positive margins. While FSA provides important insight into tumor margin status, comprehensive margin analysis of the entire sample is not practical due to the extensive time and labor required of pathologists. The limited sampling of margins in FSA and the subjective nature of tissue selection by the surgeon or pathologist remains a large opportunity to improve sampling error and identification of residual disease (4,16,17).

Besides primary tumor excision, the status of the regional LNs remains the most important negative prognostic factor for survival in patients with HNC (18–20). Up to 23% (94 of 415) of patients with HNC harbor occult nodal disease at time of diagnosis, threatening long-term survival (19,21). As a result, many patients undergo an elective neck dissection (ND) to remove all (complete ND) or many (selective ND) of the cervical LNs for cancer staging via pathology, producing a substantial pathologic burden and long-term quality of life concerns (22–25). Particular interest lies in the sentinel LN (SLN), which is the first node to which the primary tumor lymphatically drains, as staging of this node via SLN biopsy (SLNB) can be representative of the disease status of the nodal basin (ClinicalTrials.gov identifier no. NCT00275496) (26). Preoperative and intraoperative imaging focused on cancer detection and nodal staging therefore remains an integral element of the surgical resection process (27).

Near-infrared (NIR) fluorescence imaging has been widely used for decades outside of cancer treatment to

### Abbreviations

AUC = area under the receiver operating characteristic curve, EGFR = epidermal growth factor receptor, FDA = U.S. Food and Drug Administration, FGS = fluorescence-guided surgery, FLIM = fluorescence lifetime imaging, FSA = frozen-section analysis, HNC = head and neck cancer, ICG = indocyanine green, LN = lymph node, mAb = monoclonal antibody, MFI = mean fluorescence intensity, ND = neck dissection, NIR = near-infrared, PAMI = photoacoustic molecular imaging, SBR = signal-to-background ratio, SLN = sentinel LN, SLNB = SLN biopsy


### Summary

Near-infrared fluorescence-guided surgery is an intraoperative visualization technique that aids surgeons in identifying tumor margins and sentinel lymph nodes during tumor resections in patients with head and neck cancer.


### Essentials

- Antibodies and small molecules conjugated to a near-infrared (NIR) fluorescent dye allow for specific receptor targeting compared with conventional agents such as indocyanine green, which are nonspecific.
- NIR imaging with conjugated fluorophores aids in identification of tumor margins during surgery while simultaneously allowing for identification of sentinel lymph nodes and metastatic lymph nodes.
- PARPi-FL, cRGD-ZW800-1, and panitumumab-IRDye800 are agents currently in clinical trials specific to head and neck cancer focused on assessment of NIR imaging for fluorescence-guided surgery.


### Keywords

Molecular Imaging–Cancer, Fluorescence


detect tissue perfusion and outline bile duct anatomy and is now increasingly studied for diagnostic and treatment purposes in patients with cancer (12,28). Use of florescent agents in oncologic surgery was pioneered by the use of indocyanine green (ICG) in liver cancer and 5-aminolevulinic acid in glioblastoma and, in the past decade, has expanded into NIR targeted agents for use in oncologic fields, including HNC (29–34). The use of agents that create a distinction between malignant and healthy tissue in HNC would allow for real-time tumor identification and margin assessment. This review aims to provide an overview of intraoperative NIR fluorescence-guided surgery (FGS) techniques used in the clinical detection of malignant tissue and SLNs in HNC, highlighting current applications, limitations, and future directions for the use of this technology within the field.

## NIR Fluorescence

In vivo optical imaging relies on the detection of light for visualization of anatomic and physiologic differences. The surgical team's intraoperative visualization of cancerous tissue is limited by the abilities of the human eye, which can only detect light in the visible spectrum (380–700 nm). Visible light is not an attractive candidate for technological development in the surgical field, as its inability to penetrate tissue limits visualization by the human eye (10). Radiotracer agents such as technetium 99m ($^{99m}$Tc) overcome the depth issue by providing a practical penetration depth of up to 5 cm but are often limited by their spatial resolution (6–10 mm), that is, the ability to discriminate between two points emitting the same radiation. The NIR spectrum can overcome both these limitations, with a penetration depth of around 5 mm and a spatial resolution ranging from a few micrometers to 1 mm depending on the specific wavelength and tissue type (10,35,36). Beyond penetration depth, advantages of NIR fluorescence imaging include reduced autofluorescence by tissue (37) and low absorption by hemoglobin, lipids, and water as compared with other wavelengths (38). These characteristics allow for increased signal-to-background ratio (SBR) and thus improved performance as a diagnostic imaging system (10).

NIR fluorescent light is created upon the release of a photon after excitation of an NIR fluorophore at the appropriate wavelength. The emission wavelength of NIR photons ranges from 750 to 1000 nm, with the detection of these photons underlying the technique of optical fluorescence imaging (Table 1) (10). Due to the inability of the human eye to detect NIR fluorescence, specific technology is necessary to detect and translate NIR emission to white light images (10,39–42).

## Devices Used for NIR Imaging in HNC

As fluorescent imaging agents continue to advance, the development of corresponding imaging devices also remains ongoing. Typically, an imaging device is employed within the operating room, which detects the release of photons from the fluorescent imaging agent and reconstructs the signal into an image visible to the human eye, using specific filters, optical lenses, and detectors (10). There are more than a dozen devices that can be used for real-time intraoperative NIR imaging in the open field or laparoscopic/endoscopic setting (39–41). These imaging devices may be used for real-time visualization (in vivo) or specimen imaging for postexcision margin assessment on a back table (ex vivo), which is performed using black box NIR imaging devices (repurposed small animal imaging systems are the most common) (42).

Because the excitation emission spectrum for most agents being investigated overlaps with ICG, most devices used for ICG can be used for these additional NIR fluorescent probes. U.S. Food and Drug Administration (FDA)–approved devices for intraoperative ICG imaging include, but are not limited to, Stryker SPY Elite, SurgVision Explorer Air, Hamamatsu PDE-Neo, Firefly Imaging System, Quest Spectrum, Stryker PinPoint, and VisionSense Iridium. Almost all are stand-alone devices except for the Firefly Imaging System, which is integrated with the da Vinci Surgical System. Of these devices, the VisionSense Iridium and SurgVision allow for real-time overlay of white light and fluorescence images, requiring operating room light level dimmed for optimal imaging. A particular strength of all noted devices is their ability to automatically scale fluorescence, allowing only the brightest signals to be picked up. This is particularly useful in differentiating malignant LNs from benign LNs. The PDE-Neo, Quest Spectrum, and PinPoint imaging systems are handheld devices, allowing for easier use in the operating room. The remaining devices are overhead mobile systems requiring more space, which are, as expected, more expensive but provide

**Table 1: Fluorescent Agents Used for Imaging in Head and Neck Cancer and Their Properties**

| Agent | Excitation (nm) | Emission (nm) | Molecular Weight (Da) | Metabolism | Toxicity | Half-life |
|---|---|---|---|---|---|---|
| ICG | 807 | 822 | 776 | Hepatic only | Hypotension, allergic reaction, local irritation | 3–4 minutes |
| cRGDY-PEG-Cy5.5-C dots | 680 | 697 | 1069 | Hepatic only | Allergic reaction but relatively safe | Unknown |
| EGFR-targeted IRDye800CW agents | 775 | 792 | 3400 | Hepatic and renal | Hypomagnesemia, ECG changes, sinus bradycardia, elevated AST | 24–33 hours |
| CRGD-ZW800-1 | 770 | 788 | 943 | Renal only | None reported | ~3.31 hours |
| PARPi-FL | 502 | 510 | 640 | Hepatic and renal | None reported | 25–40 minutes |
| OTL38 | 776 | 796 | 29819 | Unknown | Hypertension, GI distress, allergic reaction, chest discomfort | ~86 minutes |
| ALM-488 | 490 | 525 | 2310 | Unknown | Unknown | 30 minutes |
| Nanoparticles, eg, quantum dots | | | | | | |
| Small: 2–6-nm diameter | Dependent on final coating | Dependent on size and/or payload of contrast agents | Dependent on size | Primarily renal | Composition related (based on heavy metal being used) | Dependent on composition |
| Large: >6-nm diameter | Dependent on final coating | Dependent on size and/or payload of contrast agents | Dependent on size | Primarily hepatic | Composition related (based on heavy metal being used) | Dependent on composition |

Note.—AST = aspartate aminotransferase, ECG = electrocardiogram, EGFR = epidermal growth factor receptor, GI = gastrointestinal, ICG = indocyanine green.

more sensitivity and allow for greater functionality. In vivo imaging offers valuable insights into factors like primary location, tumor margins, and unforeseen extent of disease. However, it often provides qualitative data due to uncontrollable environmental factors such as ambient light from operating room overhead lights, camera to target distance, and camera angle. Conversely, quantitative imaging data enable signal measurements and facilitate interpatient comparison. Ex vivo imaging addresses this limitation by enabling quantitative imaging within a controlled, closed-field environment. Ex vivo imaging systems have fixed camera distances and do not use ambient light, minimizing reflectance and ensuring reproducible quantitative data. For ex vivo imaging of specimens, a closed imaging system is used, with the most common being the Pearl LICOR imaging system.

ALM-488 is the only agent that does not fluoresce in the NIR wavelength and requires a separate device. Because it is being investigated to identify nerves, it requires an overhead device that allows for high magnification while also providing a stable view of fluorescent and white image overlays. The Zeiss Tivato is the most used device that fulfills all criteria, but the cost of this device is a major drawback.

## Properties of NIR Fluorescent Imaging Agents

Fluorescent contrast media leveraged for use in oncologic imaging can be generated through identification of either endogenous or exogenous fluorescence. Imaging of endogenous fluorescence in HNC includes identification of the parathyroid glands through visualization of NIR autofluorescence (at 820 nm) produced by the glands themselves. The method relies on a preliminary determination that the glands are cancerous, with the autofluorescence providing intraoperative resection guidance (43,44).

Of particular interest to this review are exogenous NIR fluorescent agents, which can be broadly categorized into agents that are activatable and those that are always on (9). Agents that are always on emit fluorescence independently of their environment, potentially resulting in a lower SBR and lower specificity (9). This category of agents is historically dominated by the FDA-approved agent ICG. A hydrophobic molecule with an absorption peak of 807 nm and an emission peak around 822 nm, ICG was first introduced in 2007 for identification of liver cancers and is now commonly used for lymphography and intraoperative angiography (Table 1) (32,45,46). ICG binds to serum proteins

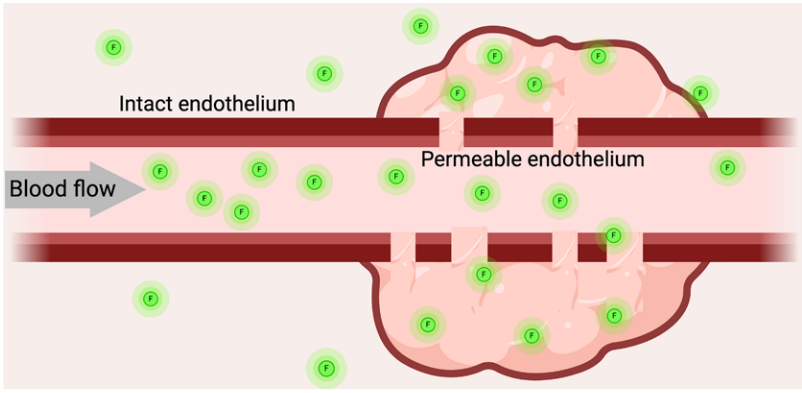


A. Non-targeted tracers such as ICG function through diffusion after binding to serum proteins. Imaging leverages the increased vascularity of tumor tissue for contrast with benign tissue.

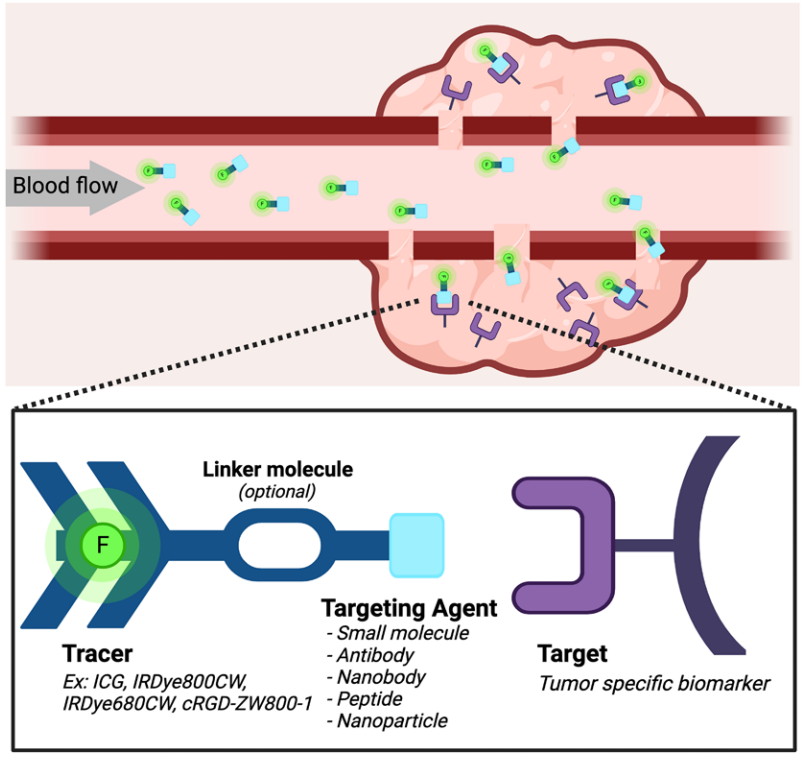


B. Targeted tracers leverage the presence of tumor specific biomarkers with the goal of decreased accumulation in benign tissue for improved contrast on imaging.

**Figure 1:** Difference in mechanism of action between nontargeted tracers and targeted tracers outlined in this article. Created with BioRender.com.

after intravenous administration, confining the fluorophore to the intravascular space. Utilizing the enhanced permeability and retention effect (47), this agent is used to nonspecifically detect cancers based on passive extravasation into tumor tissues (Fig 1) (10,12,45,48). ICG has also been used by direct injection into tumors as a reliable method of SLN mapping in patients with breast cancer and patients with melanoma since the early 2000s (49–51). The agent has been investigated this decade for use in patients with HNC for SLN mapping with and without lymphoscintigraphy (ClinicalTrials.gov identifier no. NCT02997553) and identification of parathyroid glands (52). Additional trials seek to investigate the use of the agent for detection of residual microscopic disease after primary tumor removal (ClinicalTrials.gov identifier no. NCT04842162) (53,54).

Conversely, activatable agents emit florescence depending on external factors such as environmental pH or enzymatic activity and can therefore be designed for differences in tumor-specific microenvironments. This environmental distinction gives activatable agents a potential SBR advantage over those that are always on, due to the specificity with which they emit fluorescent light (9). ONM-100 is a pH-sensitive, amphiphilic, micelle-based polymer conjugated with ICG that has been investigated for use in a variety of cancers, including HNC. On exposure to the acidic microenvironment of the tumor, the polymer dissociates, and the conjugated fluorescent dye is unquenched, allowing for emission in the NIR spectrum and subsequent visualization with the appropriate technology (Table 1) (55,56). While hypothetically more specific than always-on fluorophores, activatable fluorophores have presented challenges in achieving their specific, activated nature, potentially due to overlapping biochemical expression resulting in nonspecific signal (9).

Whether activatable or not, NIR fluorescent agents also differ in their amenability to be conjugated to a targeting molecule, providing desired specificity. This is distinct from the use of nontargeted agents, such as unconjugated ICG, which do not bind to or interact with tumor-specific molecules. The rapid development of targeted tracers consisting of an imaging moiety conjugated to a tumor-specific targeting agent have been explored in the past decade to improve identification of primary solid tumors (Fig 1) (57,58). Targeted agents leverage the fact that certain cell populations express unique biomarkers (58). Probes such as small peptides, antibodies, and inorganic nanoparticles can be designed to target markers overexpressed by tumor cells, allowing for a dynamic, individualized approach to tracer administration (59,60). The surge of research into targeted fluorescent tracers for FGS was initiated in the early 2010s with trials focused on both breast cancer and HNC (ClinicalTrials.gov identifier nos. NCT01508572 and NCT01987375). Today, many of the targeted agents currently under investigation provide a variety of valuable features, including high affinity and avidity for the target, rapid penetration into the tumor, and decreased accumulation within normal (benign) tissues to allow for sufficient contrast for improved visualization (12,61,62).

**Table 2: Clinical Trials Cited in This Article Involving Fluorescent Agents for Use in Head and Neck Cancer Treatment**

| Trial/Status | Agent | Tracer Type | Target |
|---|---|---|---|
| NCT02997553/Completed | ICG | Fluorescent dye | NA |
| NCT04842162/Recruiting | ICG | Fluorescent dye | NA |
| NCT01987375/Terminated | Cetuximab-IRDye800 | Fluorescent-labeled mAb | EGFR |
| NCT03134846/Recruiting | Cetuximab-IRDye800 | Fluorescent-labeled mAb | EGFR |
| NCT03923881/Recruiting | Cetuximab-IRDye800 | Fluorescent-labeled mAb | EGFR |
| NCT02415881/Completed | Panitumumab-IRDye800 | Fluorescent-labeled mAb | EGFR |
| NCT04511078/Recruiting | Panitumumab-IRDye800 | Fluorescent-labeled mAb | EGFR |
| NCT03085147/Recruiting | PARPi-Fl | Fluorescent-labeled small molecule | PARP-1 |
| NCT04191460/Not yet recruiting | cRGD-ZW800-1 | Fluorescent protein | Integrin |
| NCT02106598/Recruiting | Fluorescent cRGDY-PEG-Cy5.5-C dots | Fluorescent-labeled nanoparticle | Integrin |
| NCT03733210/Completed | Panitumumab-IRDye800 and 89Zr-Panitumumab | Fluorescent- and radiolabeled mAb | EGFR |
| NCT05377554/Recruiting | ALM-488 | Fluorescent-labeled peptide | Extracellular matrix of nerves |

Note.—EGFR = epidermal growth factor receptor, ICG = indocyanine green, mAb = monoclonal antibody, NA = not applicable, PARP-1 = poly [ADP-ribose] polymerase 1.

## Implementation of NIR Fluorescent Agents in HNC Surgery

With the clinical promise of targeted NIR agents for intraoperative imaging in HNC, this review evaluates the current landscape of their use in oncologic HNC FGS.

Current clinical trials investigating the use of NIR fluorescent imaging agents for HNC surgical imaging follow broadly similar protocols (11,16,25,63–68) (Table 2). Intravenous administration of the imaging agent is followed by a period of 0–5 days prior to surgery, allowing for dispersion of the agent within the body. This period is dependent on the half-life of the agent and the determined time frame during which the SBR will be highest. Patients then undergo standard-of-care tumor resection involving surgical removal of malignant tissue, which is most often located in the oral cavity, oropharynx, hypopharynx, and supraglottis. Depending on suspicion for nodal metastasis, lymphadenectomy may be pertinent, requiring removal of the LNs within the cervical nodal basins. Throughout the surgery, fluorescence imaging is performed either in vivo, with open-field imaging devices, or ex vivo, with open- or closed-field imaging devices (Fig 2). In vivo analysis involves imaging of the tumor prior to completed resection once superficial tissue has been resected and after tumor excision for wound bed imaging. Ex vivo imaging involves use of either open-field or closed-field devices to measure fluorescence of the tumor specimen after excision for mapping and margin assessment. This may happen on the back table during the surgical procedure or following surgical completion (Fig 2). Current trials aim to demonstrate that FGS not only maintains standard-of-care surgical treatment in HNC, but can also aid in tumor localization and delineation, potentially altering postoperative decision-making.

## Applications of NIR Agents in HNC

Use of in vivo NIR imaging in the surgical management of HNC can be generally subdivided into categories based on the desired outcome of the imaging: *(a)* localization of diseased tissue during primary tumor removal (in situ), *(b)* wound bed assessment after primary tumor removal, *(c)* ex vivo analysis of the "sentinel margin," and *(d)* identification of the SLN and metastatic LNs (Fig 3).

## FGS for Primary Tumor Identification and Margin Evaluation

Due to the necessity of complete tumor removal for long-term patient survival, localization of tumor tissue and attainment of precise negative margins were the focus of early NIR FGS investigations. Initial studies involved fluorophores conjugated to monoclonal antibodies (mAbs), with some investigation into conjugated small molecules and peptides (11,16,63–65,69) (Table 1). Trials leveraged known safety profiles of mAbs, such as cetuximab-IRDye800, an mAb covalently linked to the NIR fluorophore IRDye800CW (ClinicalTrials.gov identifier no. NCT03134846) (Tables 1, 2) (64,65). Cetuximab targets the epidermal growth factor receptor (EGFR), which is a transmembrane cell surface glycoprotein overexpressed by more than 90% (22 of 24) of head and neck squamous cell carcinomas, making it a valuable target for therapies and imaging agents alike (16). While these studies demonstrated the potential of cetuximab-IRDye800 for in situ tumor identification and margin assessment via analysis of SBR fluorescent signal, future studies increasingly investigated panitumumab-IRDye800 due to the agent's more promising safety profile and higher binding affinity with EGFR (70).

For panitumumab-IRDye800 trials in primary tumor localization and margin analysis, open-field imaging systems are used

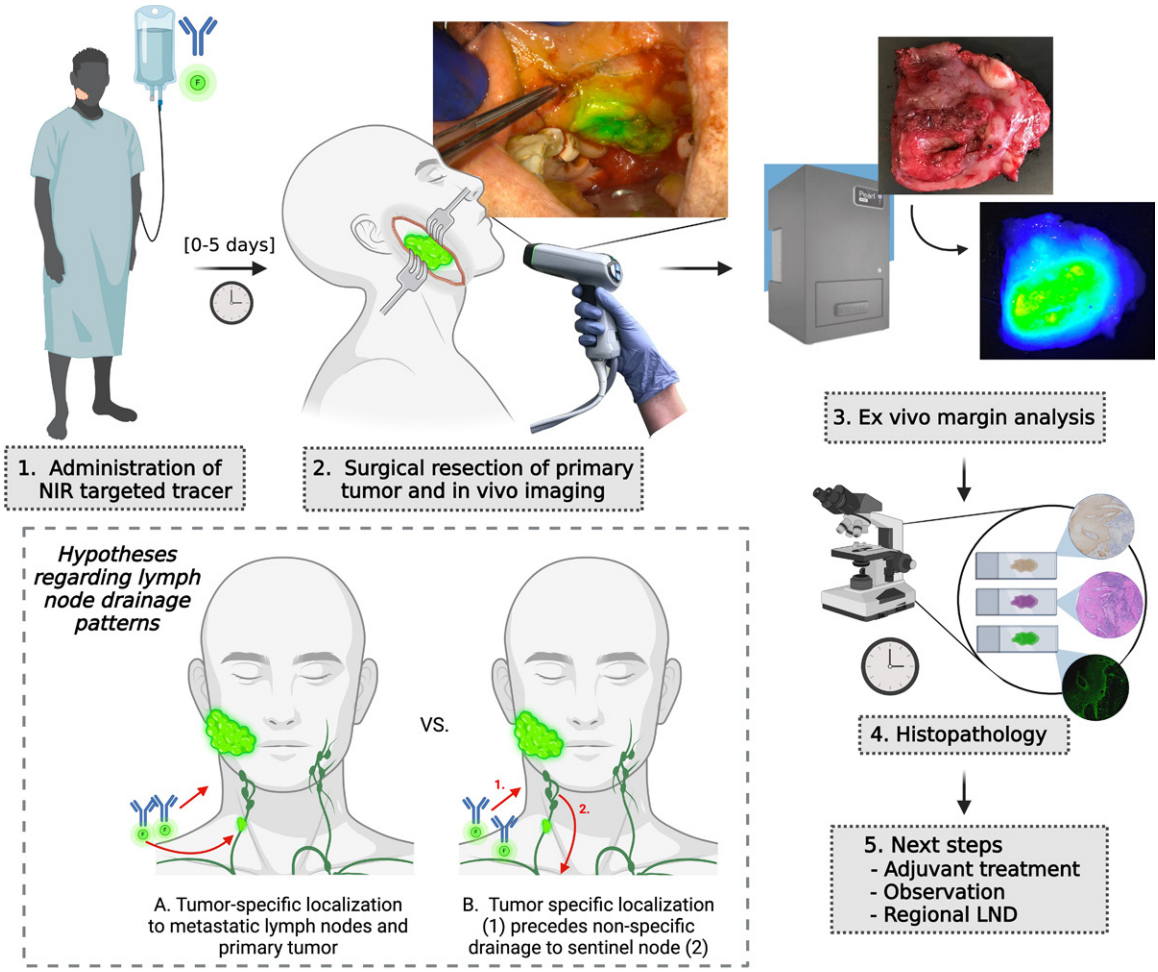


**Figure 2:** Workflow for targeted tracer in primary tumor and metastatic lymph node detection. LND = lymph node dissection, NIR = near-infrared. Created with BioRender.com.

to guide resection of the primary tumor—particularly the deep margin (defined as the distance between the tumor border and the cut edge of the specimen on the deep side of the tumor)—and identify secondary satellite lesions originally missed by standard-of-care methods. The end goal of FGS is to improve surgical decision-making, which can be defined as the surgical team changing their management plan based on findings from FGS. A phase 1 clinical trial involving panitumumab-IRDye800 that analyzed data from 20 different patients for in situ tumor imaging (ClinicalTrials.gov identifier no. NCT02415881) found that SBR was significantly higher in tumor-positive tissue than tumor-negative tissue during preresection imaging of the surgical area, ranging from 1.5 to 2.9 (average, 2.2 ± 0.4) (11). Moreover, in situ imaging of the wound cavity after resection resulted in an SBR below 1, suggesting a negative margin, as wound bed fluorescence was lower than that of background tissue. This was supported by the lack of positive margins at final pathology (63). The real strength of the technique was observed when one of the patients in this trial had a positive deep margin that was missed by the surgical team but picked up with the in situ imaging system. On further deep margin analysis with an ex vivo imaging system using the resected primary specimen, the presence of a close margin was accurately predicted, with increased fluorescent signal detected on the surface of the resected tumor, which was later found to have a close margin of 3.8 mm (63). In the same trial, one patient had a secondary satellite lesion that was missed at preoperative imaging. On inspection with in situ imaging, the secondary lesion was found before the incision, and the surgical team modified their incision to remove the secondary satellite lesion as well. Final pathologic evaluation of the second lesion revealed an invasive squamous cell carcinoma that was separated from the primary tumor by a bridge of 4.2-mm normal mucosa. The use of this technology for in situ imaging may have the potential to provide surgical teams with an additional modality for real-time tumor detection during operations, offering an additional layer of information to inform surgical decision-making. The study by Van Keulen et al (63) showed that FGS guided surgical decision-making in 21.4% (three of 14) of patients. A current clinical trial seeks to continue this work by comparing fluorescence intensity of tumor tissue to that of normal surrounding tissue after administration of panitumumab-IRDye800 (ClinicalTrials.gov identifier no. NCT04511078) (Table 2).

While in situ fluorescence imaging provides supportive information for the surgical team, the difficult imaging conditions of HNC due to the deep and narrow wound beds and limited exposure of tumor support the use of ex vivo tumor mapping as

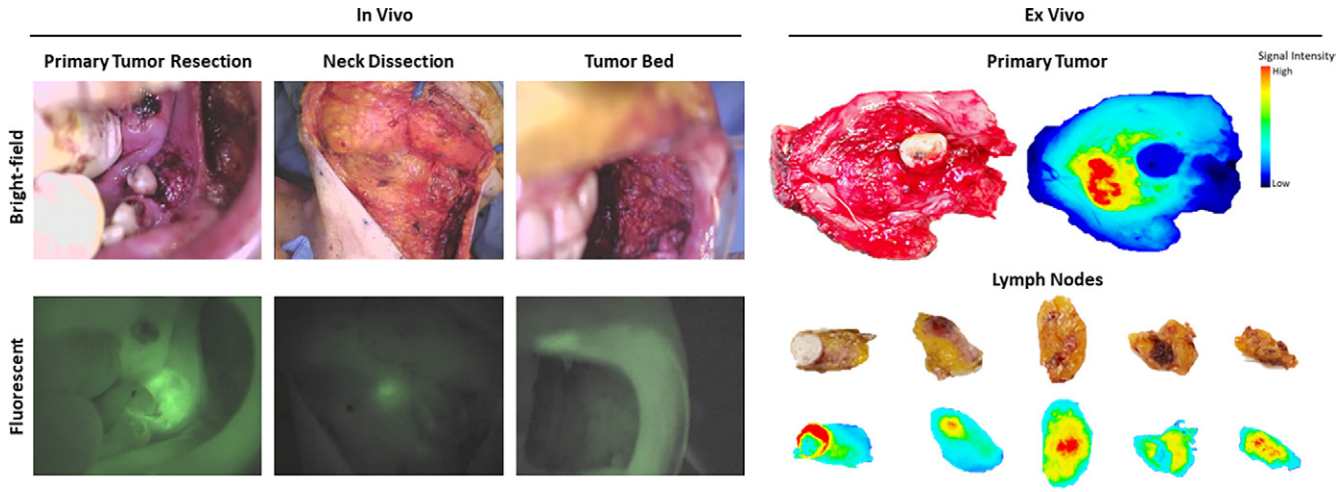


**Figure 3:** Application of near-infrared imaging for assessment of tumor, lymph nodes, and tumor bed after resection.

a guidance system for pathologic margin assessment (16). Although FSA has an accuracy of 95% (90 of 3697) when performed by an experienced pathologist, only a small proportion of the specimen may be sampled, potentially contributing to the high rates of positive margins in HNC (43,71). Published results from our trial using panitumumab-IRDye800 (ClinicalTrials.gov identifier no. NCT 02415881) demonstrate a correlation between high fluorescent signal in ex vivo tumor imaging and specimen regions with the highest probability of having a close margin during pathology (72). This technology can be applied more broadly to "map" the tumor, which involves creating an ex vivo, three-dimensional image of the entire tumor specimen with a closed-field imaging device. Ex vivo fluorescent specimen mapping to predict positive margins (<5 mm) showed high sensitivity (95%) and specificity (89%), with an area under the receiver operating characteristic curve (AUC) of 0.97 (71). Moreover, subsequent histopathology showed that fluorescence intensity correlated with closer histopathologic margin distances (72,73). Identification of positive margins using fluorescence intensity has been demonstrated by other groups as well, with high sensitivity and specificity (65,74,75). One caveat, however, is sparsity of data regarding the effect of prior radiation or surgery on the SBRs for margin analysis. Fibrosis at the site of treatment might alter signal, but this is not yet proven and remains an area of unmet research. A recent study published using EGFR-targeted fluorescence to identify intraoperative margins included 19 patients who had undergone prior surgery and 20 patients who had undergone prior radiation therapy. There was no evidence of a statistically significant difference in the intrinsic fluorescence of tissue that was radiated compared with nonradiated tissue. Similar results were found for ICG when it was used to detect SLNs in patients who underwent radiation therapy for nasopharyngeal carcinoma. Although there were only nine patients enrolled in the trial, the authors stated that previous radiation therapy did not hinder identification of SLNs (76).

Additional investigation into agents used for localization and margin evaluation of primary tumors in HNC include topically administered PARPi-FL, an NIR small molecule–targeting poly [ADP-ribose] polymerase 1 (PARP1) used in the detection of oral cancer (69) (ClinicalTrials.gov identifier no. NCT03085147), and NIR cRGD-ZW800-1, targeting integrin (ClinicalTrials.gov identifier no. NCT04191460) (Tables 1, 2). PARPi-FL is of particular interest as it is applied topically and can be simply gargled by the patient prior to the procedure, allowing for improved workflow in the surgical space. Early trials have demonstrated that a dose of 1000 nM results in tumor to margin fluorescent signals of more than three in ex vivo tumor imaging (66). While topical administration is advantageous in many settings, it may fall short in patients with more deeply embedded malignancies. Results of trials involving use of NIR cRGD-ZW800-1 in HNC are yet to be released, but studies in animal models demonstrate promising results (77).

## FGS for Metastatic and Sentinel LN Detection

The issue of occult metastatic nodal disease in patients with HNC remains paramount in treatment decisions. Even when using more sensitive immunohistochemical and molecular techniques, studies have found undetected micro metastatic disease in 5%–58% (mean of 19.6%) of initially pathologically negative neck nodal specimens (78). Current standard of care for patients with HNC involves a complete or selective ND, where all or many of the cervical LNs are removed due to concern for occult nodal disease. In an effort to capture the occult metastatic spread to LNs, 70%–80% of patients are overtreated and undergo ND only for a lack of cervical nodal disease to be found at pathology, highlighting the delicate balance between ensuring removal of metastatic LNs and avoiding excessive tissue removal (19). Another issue arises when LNs have extracapsular spread of disease, which substantially worsens prognosis (79). Because the disease often spreads into surrounding musculature, it becomes very arduous to distinguish between normal tissue versus diseased tissue and makes dissecting the disease very challenging. These rates, along with the morbidity associated with ND, suggest movement toward the use of SLNB, which is considered standard of care in breast cancer, melanoma, and HNC in many European countries (19,21,80). Limitations such as presence of multiple lymphatic drainage

patterns in the head and neck region result in a technically challenging and time-consuming SLNB (81). Although a prospective, randomized trial seeks to compare quality of life and oncologic outcomes between SLNB and ND in early-stage oral cavity cancers (ClinicalTrials.gov identifier no. NCT04333537), there continues to be a need for improved workflow in HNC treatment. Fluorescent tracers show potential in supporting decision-making during ND and SLNB.

In studies involving systemic administration of either cetuximab-IRDye800 or panitumumab-IRDye800, a significant difference was found in the mean fluorescence intensity (MFI) between tumor-positive and tumor-negative LNs (25,66,67). When ranked by fluorescence intensity, fluorescence predicted metastatic nodes in patients with clinically node-negative disease, with 100% sensitivity, 85.8% specificity, and 100% negative predictive value (25). When MFI and SBR were combined, a 0.6% false-negative rate was identified, indicating potential for use in preselection of at-risk LNs (66). Moreover, in two studies using cetuximab-IRDye800CW, 7%–8% of samples initially thought to be tumor negative were later determined to be tumor positive at histopathology, which corresponded to ex vivo positive fluorescent signal, altering the staging of two patients per study (67,68). These results indicate the ability of FGS agents to contribute to pathologic decision-making, including the ability to decrease the number of LNs requiring histopathologic examination by 77.4% (67). In another study, a patient's preoperative MRI findings revealed a suspicious LN and an indistinct mass in level II of the right neck, as well as a suspicious LN in level V of the right neck. PET imaging only disclosed a solitary fluorine 18 fluorodeoxyglucose–avid spot in level II that was positive at fine-needle aspiration. Intraoperative fluorescence imaging demonstrated several fluorescent LNs in level II, as well as the level V LN that was observed at preoperative MRI. Repeated fluorescence imaging was particularly valuable for visualization of the extent of the level II mass, which was found to have infiltrated the deep neck musculature. At complete gross resection of this mass, it was found that fluorescence imaging allowed for the identification of multiple small pieces of residual tissue that were not detected by the surgeon's gross inspection (63). Pathologic assessment of these tissue samples with FSA confirmed squamous cell carcinoma. FGS also provides value when compared with conventional SLN identification through peritumoral $^{99m}$Tc-tilmanocept. A study by Krishnan et al (25) compared two patients who received both panitumumabIRDye800 and peritumoral $^{99m}$Tc-tilmanocept. In patient 1, preoperative scans revealed two SLN clusters that were also identified intraoperatively with a γ-ray probe. These SLN clusters had the highest γ counts and MFI intensity at fluorescence imaging. However, in patient 2, one SLN cluster was identified preoperatively that was also picked up by the γ-ray probe intraoperatively. Interestingly, this SLN cluster did not show much signal at intraoperative fluorescence imaging. Once an elective ND was performed, this SLN cluster turned out to be benign; however, two additional LNs were identified at pathologic analysis that had macrometastasis and the highest MFI at fluorescence imaging, even more so than the SLN. These LNs were missed with conventional radionuclide techniques. This suggests that the injection may have been performed in a manner that did not accurately identify the SLN and highlights the advantage of FGS, which removes the variability associated with peritumoral radionuclide injection, which can be very painful and challenging in some patients. Investigations into alternative imaging devices (ClinicalTrials.gov identifier no. NCT03923881), alternative agents such as NIR cRGD-ZW800–1 (ClinicalTrials.gov identifier no. NCT04191460) and cRGDY-PEG-Cy5.5, targeting integrin (ClinicalTrials.gov identifier no. NCT02106598) (82), and dual-tracer technology (ClinicalTrials.gov identifier no. NCT03733210) indicate continued interest in the expansion of this technology in HNC management (Tables 1, 2).

The mechanism by which the tracer localizes to metastatic LNs is still under investigation. The correlation between metastatic tissue and fluorescent signal suggests that the agent may specifically localize to diseased tissue in the LNs due to the targeting specificity of the agent. However, pathologic findings demonstrate concentration of the agent in the periphery of the lymphatic tissue, likely due to passive lymphatic flow, suggesting accumulation after nonspecific drainage from the primary tumor (66). Additional indications that the agent preferentially reaches the SLN via nonspecific drainage include the following: *(a)* the increase in false-positive LNs with increased dose of panitumumab-IRDye800 (64) and *(b)* the false-positive LNs identified by fluorescent signal after systemic administration of panitumumab-IRDye800 (25). If these targeted agents follow nonspecific drainage patterns similar to agents injected directly into the tumor, the benefit of systemic administration creates an avenue for improved standard-of-care workflow due to the inaccessible nature of some HNC primary tumors, such as those in the larynx or hypopharynx, for peritumoral injection (83). Additionally, by avoiding painful and complicated peritumoral injections in sensitive locations, such as the tongue or posterior oropharynx, intravenous administration of imaging agents has broad implications for decreasing morbidity associated with the already complex treatment of patients with HNC.

## Challenges

While many advantages of FGS in HNC exist, the drawbacks of the targeted agents have prevented the widespread adoption of their use. Physical limitations include the penetration depth of the NIR fluorophores, which remain close to 5 mm. This compares poorly to US-guided intraoperative tumor assessment, which has been determined to effectively delineate tumor depth up to 7 mm during intraoperative imaging, with strong correlation with histopathologic measurements of both tumor thickness and depth of invasion (14,15). Moreover, while fluorescent agents may identify tumor tissue at shallow depths (0–5 mm), they cannot provide a complete picture of disease in large specimens or those covered by healthy tissue (>10 mm) (16). For in vivo imaging, the tumor must be well exposed, meaning that the surgeon must know where to look before resection and imaging take place. This is particularly problematic when trying to

identify LNs that are buried deep within the neck (ie, retropharyngeal LNs). Because these LNs are usually several centimeters deep in the neck, FGS usually fails to detect them unless extensive dissection is done. There is also a paucity of data with regard to identification of retropharyngeal LNs through FGS, as metastasis to the retropharyngeal LNs is an indication for nonoperative treatment modalities. In ex vivo imaging, the 5-mm penetration drawback impacts imaging reliability, particularly of large specimens.

Fluorescence intensity is also impacted by the concentration of the agent, the autofluorescence of local tissue, and both the imaging device sensitivity (due to the variable selection of devices) and user technique (9). As these differ across trial and patient, comparing results presents unique challenges (84). As previously mentioned, imaging devices differ among institutions, with a multitude of handheld devices or stand-alone systems present for use. This makes it extremely challenging to standardize results across trials. Furthermore, the exuberant costs of these devices limit their availability in certain treatment centers.

Drawbacks in clinical translation are framed broadly around procedural, regulatory, and trial end point challenges. Because most agents used in FGS are based on an mAb backbone, they necessitate intravenous administration primarily due to their large molecular weight and intricate structure, rendering them poorly absorbable via oral routes. Moreover, as antibodies take time to dissipate through the blood to their target antigen, patients often need to be given the agent 24–48 hours before surgery; this necessitates another hospital visit, which is impractical for patients who must travel long distances for each visit. Additionally, as antibody-based fluorescent agents are also subject to the enhanced permeability and retention effect, there is nonspecific uptake in tumors, which makes it necessary to wait after drug administration for unbound drug to clear from tumors and not cause autofluorescence. Furthermore, competing technologies slow the advancement of the field, as each must proceed independently through the regulatory process rather than building methodically on past work (9). Current clinical trials and published studies lack assessment of the objective applicability of the technology. Focus remains on comparison of fluorescence in diseased tissue and healthy tissue, rather than investigation into how better to integrate the technology with current surgical systems. Creating standard protocols across institutions will aid in evaluating how these new objective technologies can be added to subjective and varying surgeon experience and expertise. Specifically, in vivo imaging is difficult to compare, as surgeons make subjective decisions regarding images generated in real time. Thus, results are impacted by surgeon training, perspective, and non–image-based sensory input. Streamlining protocols with a focus on integration into the current surgical setting will focus future research in a manner that allows for methodical evaluation (85).

## Future Directions

With the demonstrated promise of NIR agents for use at FGS in HNC, future directions of the field involve continued research into molecular targeted tracers more broadly. Within HNC, molecularly targeted NIR tracers are being combined with molecularly targeted radiotracers (ClinicalTrials.gov identifier no. NCT03733210) for a dual-targeting system already investigated in animal models (86). Radiotracers combine a molecular targeting agent (such as panitumumab) with a radioisotope (such as zirconium 89), allowing for both preoperative imaging via PET or SPECT and intraoperative localization of tumor tissue via NIR fluorescence. These combination tracers have potential for increased penetration depth, which is a limitation of NIR agents as previously mentioned in this review. Also, there are currently ongoing trials looking at infusing both panitumumab-IRDye800 and indium 11 panitumumab ($^{111}$In-panitumumab) to better identify LNs preoperatively and intraoperatively (ClinicalTrials.gov identifier no. NCT05945875). The current issue with nonspecific radionuclides is that they still require an elective ND in cN0 disease to confirm whether an LN is malignant or not. Using panitumumab-specific radiotracers would help clinicians better identify positive LNs and decide whether a morbid procedure such as an elective ND is truly needed. Moreover, because $^{111}$In-panitumumab is injected intravenously, it overcomes some of the limitations associated with conventional radionuclide techniques in HNC. The intraoperative identification of vital, nontumor tissues is being investigated using the fluorescent nerve-targeting agent ALM-488 to more clearly visualize nerves encountered during ND, parotidectomy, and thyroidectomy (ClinicalTrials.gov identifier no. NCT05377554) (87). With the FDA approval of pafolacianine (Cytalux), a folate-targeting NIR imaging agent (OTL38) for use in patients with ovarian cancer, the expansion of targeted NIR imaging agents across cancer types is promising (Tables 1, 2).

Outside of agents themselves, imaging techniques present additional promise, with photoacoustic molecular imaging (PAMI), a hybrid technology combining US and optical imaging, on the forefront. PAMI uses laser irradiation to create ultrasonic waves that are detected via standard US transducers. When combined with fluorescence imaging, PAMI demonstrates high-resolution imaging of depths up to 5 cm (88). Studies using panitumumab-IRDye800CW for ex vivo identification of metastatic LNs demonstrate highly accurate differentiation between normal and occult LNs (AUC 0.96) (89). Another interesting imaging modality is fluorescence lifetime imaging (FLIM). Unlike traditional fluorescence imaging, which captures the intensity of emitted light, FLIM focuses on the time it takes for the fluorescence to return to the ground state, known as the fluorescence lifetime. This lifetime is the characteristic time that a fluorophore remains in its excited state before emitting a photon and returning to its ground state. A study using FLIM on specimens from patients injected with panitumumab-IRDye800 reported an AUC of 0.98 for FLIM-based tumor/normal classification compared with an AUC of 0.32 for traditional intensity-based classification. FLIM values also tended to better correlate with EGFR expression by immunohistochemistry ($r$ = 0.85) compared with traditional signal intensity values ($r$ = –0.12) (90). Other current research is exploring additional techniques like fluorescence confocal endomicroscopy, which

delivers high-resolution live imaging of cellular structures within deep tissues. This method employs a confocal strategy to remove out of focus light, thus improving image clarity at multiple depths. Additionally, NIR-II window imaging is being investigated for its use of NIR light in the 1000–1700 nm spectral range. This approach allows for greater tissue penetration and minimizes autofluorescence, providing clearer and more detailed images suitable for in vivo research and potential clinical use. Further investigation into these imaging modalities may prove insightful in determining optimal imaging techniques for targeted NIR fluorescent agents in HNC resection and nodal dissection.

## Conclusion

The clinical impact of FGS in HNC extends beyond the identification of tumor for surgical removal. Postoperative care is highly dependent on the results of surgical proceedings and the staging of the patient. Thus, more accurate identification of the extent of disease has the potential to not only improve removal of diseased tissue but also improve decision-making regarding adjuvant therapy options. Research into the effectiveness of cancer immunotherapy after nodal dissection highlights the need for improved differentiation between metastatic and benign nodes (91). As such, the field of FGS in HNC would benefit from further, organized research into additional agents and imaging systems, with particular focus on a structured method that would allow for better interstudy comparisons.

**Disclosures of conflicts of interest:** **H.W.W.** No relevant relationships. **A.B.N.** No relevant relationships. **B.R.C.** No relevant relationships. **Y.J.L.** No relevant relationships. **F.M.B.** No relevant relationships. **M.T.** No relevant relationships. **E.L.R.** No relevant relationships. **M.E.H.** No relevant relationships.

## References

1. Atallah I, Milet C, Coll JL, Reyt E, Righini CA, Hurbin A. Role of near-infrared fluorescence imaging in head and neck cancer surgery: from animal models to humans. Eur Arch Otorhinolaryngol 2015;272(10):2593–2600.
2. Binahmed A, Nason RW, Abdoh AA. The clinical significance of the positive surgical margin in oral cancer. Oral Oncol 2007;43(8):780–784.
3. Eldeeb H, Macmillan C, Elwell C, Hammod A. The effect of the surgical margins on the outcome of patients with head and neck squamous cell carcinoma: single institution experience. Cancer Biol Med 2012;9(1):29–33.
4. Wu C, Gleysteen J, Teraphongphom NT, Li Y, Rosenthal E. In-vivo optical imaging in head and neck oncology: basic principles, clinical applications and future directions. Int J Oral Sci 2018;10(2):10.
5. Ravasz LA, Slootweg PJ, Hordijk GJ, Smit F, van der Tweel I. The status of the resection margin as a prognostic factor in the treatment of head and neck carcinoma. J Craniomaxillofac Surg 1991;19(7):314–318.
6. Mitchell DA, Kanatas A, Murphy C, Chengot P, Smith AB, Ong TK. Margins and survival in oral cancer. Br J Oral Maxillofac Surg 2018;56(9):820–829.
7. Payakachat N, Ounpraseuth S, Suen JY. Late complications and long-term quality of life for survivors (>5 years) with history of head and neck cancer. Head Neck 2013;35(6):819–825.
8. Orosco RK, Tapia VJ, Califano JA, et al. Positive Surgical Margins in the 10 Most Common Solid Cancers. Sci Rep 2018;8(1):5686.
9. Lee YJ, Krishnan G, Nishio N, et al. Intraoperative Fluorescence-Guided Surgery in Head and Neck Squamous Cell Carcinoma. Laryngoscope 2021;131(3):529–534.
10. de Boer E, Harlaar NJ, Taruttis A, et al. Optical innovations in surgery. Br J Surg 2015;102(2):e56–e72.
11. van Keulen S, Nishio N, Fakurnejad S, et al. Intraoperative Tumor Assessment Using Real-Time Molecular Imaging in Head and Neck Cancer Patients. J Am Coll Surg 2019;229(6):560–567.e1.
12. Gibbs SL. Near infrared fluorescence for image-guided surgery. Quant Imaging Med Surg 2012;2(3):177–187.
13. Hussain T, Nguyen QT. Molecular imaging for cancer diagnosis and surgery. Adv Drug Deliv Rev 2014;66:90–100.
14. Yoon BC, Bulbul MD, Sadow PM, et al. Comparison of Intraoperative Sonography and Histopathologic Evaluation of Tumor Thickness and Depth of Invasion in Oral Tongue Cancer: A Pilot Study. AJNR Am J Neuroradiol 2020;41(7):1245–1250.
15. Di Meo G, Prete FP, De Luca GM, et al. The Value of Intraoperative Ultrasound in Selective Lateral Cervical Neck Lymphadenectomy for Papillary Thyroid Cancer: A Prospective Pilot Study. Cancers (Basel) 2021;13(11):2737.
16. Gao RW, Teraphongphom NT, van den Berg NS, et al. Determination of tumor margins with surgical specimen mapping using near-infrared fluorescence. Cancer Res 2018;78(17):5144–5154.
17. Preeti A, Sameer G, Kulranjan S, et al. Intra-operative frozen sections: Experience at a tertiary care centre. Asian Pac J Cancer Prev 2016;17(12):5057–5061.
18. Mamelle G, Pampurik J, Luboinski B, Lancar R, Lusinchi A, Bosq J. Lymph node prognostic factors in head and neck squamous cell carcinomas. Am J Surg 1994;168(5):494–498.
19. Civantos FJ, Zitsch RP, Schuller DE, et al. Sentinel lymph node biopsy accurately stages the regional lymph nodes for T1-T2 oral squamous cell carcinomas: results of a prospective multi-institutional trial. J Clin Oncol 2010;28(8):1395–1400.
20. Dogan NU, Dogan S, Favero G, Köhler C, Dursun P. The Basics of Sentinel Lymph Node Biopsy: Anatomical and Pathophysiological Considerations and Clinical Aspects. J Oncol 2019;2019:3415630.
21. Schilling C, Stoeckli SJ, Haerle SK, et al. Sentinel European Node Trial (SENT): 3-year results of sentinel node biopsy in oral cancer. Eur J Cancer 2015;51(18):2777–2784.
22. D'Cruz AK, Vaish R, Kapre N, et al; Head and Neck Disease Management Group. Elective versus Therapeutic Neck Dissection in Node-Negative Oral Cancer. N Engl J Med 2015;373(6):521–529.
23. Hiraki A, Fukuma D, Nagata M, et al. Sentinel lymph node biopsy reduces the incidence of secondary neck metastasis in patients with oral squamous cell carcinoma. Mol Clin Oncol 2016;5(1):57–60.
24. Martin H, Del Valle B, Ehrlich H, Cahan WG. Neck dissection. Cancer 1951;4(3):441–499.
25. Krishnan G, van den Berg NS, Nishio N, et al. Metastatic and sentinel lymph node mapping using intravenously delivered Panitumumab-IRDye800CW. Theranostics 2021;11(15):7188–7198.
26. Bello DM, Faries MB. The Landmark Series: MSLT-1, MSLT-2 and DeCOG (Management of Lymph Nodes). Ann Surg Oncol 2020;27(1):15–21.
27. Frangioni JV. New technologies for human cancer imaging. J Clin Oncol 2008;26(24):4012–4021.
28. Kosaka N, Ogawa M, Choyke PL, Kobayashi H. Clinical implications of near-infrared fluorescence imaging in cancer. Future Oncol 2009;5(9):1501–1511.
29. Stummer W, Stocker S, Wagner S, et al. Intraoperative detection of malignant gliomas by 5-aminolevulinic acid-induced porphyrin fluorescence. Neurosurgery 1998;42(3):518–525; discussion 525–526.
30. Stummer W, Pichlmeier U, Meinel T, Wiestler OD, Zanella F, Reulen HJ; ALA-Glioma Study Group. Fluorescence-guided surgery with 5-aminolevulinic acid for resection of malignant glioma: a randomised controlled multicentre phase III trial. Lancet Oncol 2006;7(5):392–401.
31. Georges JF, Valeri A, Wang H, et al. Delta-Aminolevulinic Acid-Mediated Photodiagnoses in Surgical Oncology: A Historical Review of Clinical Trials. Front Surg 2019;6:45.
32. Ishizawa T, Fukushima N, Shibahara J, et al. Real-time identification of liver cancers by using indocyanine green fluorescent imaging. Cancer 2009;115(11):2491–2504.
33. Purich K, Dang JT, Poonja A, et al. Intraoperative fluorescence imaging with indocyanine green in hepatic resection for malignancy: a systematic review and meta-analysis of diagnostic test accuracy studies. Surg Endosc 2020;34(7):2891–2903.
34. Lauwerends LJ, van Driel PBAA, Baatenburg de Jong RJ, et al. Real-time fluorescence imaging in intraoperative decision making for cancer surgery. Lancet Oncol 2021;22(5):e186–e195.
35. Vahrmeijer AL, Hutteman M, van der Vorst JR, van de Velde CJH, Frangioni JV. Image-guided cancer surgery using near-infrared fluorescence. Nat Rev Clin Oncol 2013;10(9):507–518.
36. Chance B. Near-infrared images using continuous, phase-modulated, and pulsed light with quantitation of blood and blood oxygenation. Ann N Y Acad Sci 1998;838(1):29–45.
37. Zhu B, Rasmussen JC, Lu Y, Sevick-Muraca EM. Reduction of excitation light leakage to improve near-infrared fluorescence imaging for tissue surface and deep tissue imaging. Med Phys 2010;37(11):5961–5970.

38. Gibson AP, Hebden JC, Arridge SR. Recent advances in diffuse optical imaging. Phys Med Biol 2005;50(4):R1–R43.
39. Muallem MZ, Sayasneh A, Armbrust R, Sehouli J, Miranda A. Sentinel lymph node staging with indocyanine green for patients with cervical cancer: The safety and feasibility of open approach using spy-phi technique. J Clin Med 2021;10(21):4849.
40. Petz W, Bertani E, Borin S, Fiori G, Ribero D, Spinoglio G. Fluorescence-guided D3 lymphadenectomy in robotic right colectomy with complete mesocolic excision. Int J Med Robot 2021;17(3):e2217.
41. Boni L, David G, Dionigi G, Rausei S, Cassinotti E, Fingerhut A. Indocyanine green-enhanced fluorescence to assess bowel perfusion during laparoscopic colorectal resection. Surg Endosc 2016;30(7):2736–2742.
42. DSouza AV, Lin H, Henderson ER, Samkoe KS, Pogue BW. Review of fluorescence guided surgery systems: identification of key performance capabilities beyond indocyanine green imaging. J Biomed Opt 2016;21(8):80901.
43. Olson SM, Hussaini M, Lewis JS Jr. Frozen section analysis of margins for head and neck tumor resections: reduction of sampling errors with a third histologic level. Mod Pathol 2011;24(5):665–670.
44. Ladurner R, Lerchenberger M, Al Arabi N, Gallwas JKS, Stepp H, Hallfeldt KKJ. Parathyroid Autofluorescence-How Does It Affect Parathyroid and Thyroid Surgery? A 5 Year Experience. Molecules 2019;24(14):2560.
45. Schaafsma BE, Mieog JSD, Hutteman M, et al. The clinical use of indocyanine green as a near-infrared fluorescent contrast agent for image-guided oncologic surgery. J Surg Oncol 2011;104(3):323–332.
46. van Leeuwen FWB, Hardwick JCH, van Erkel AR. Luminescence-based imaging approaches in the field of interventional molecular imaging. Radiology 2015;276(1):12–29.
47. Zhang RR, Schroeder AB, Grudzinski JJ, et al. Beyond the margins: real-time detection of cancer using targeted fluorophores. Nat Rev Clin Oncol 2017;14(6):347–364.
48. Yoneya S, Saito T, Komatsu Y, Koyama I, Takahashi K, Duvoll-Young J. Binding properties of indocyanine green in human blood. Invest Ophthalmol Vis Sci 1998;39(7):1286–1290.
49. Xiong L, Gazyakan E, Yang W, et al. Indocyanine green fluorescence-guided sentinel node biopsy: a meta-analysis on detection rate and diagnostic performance. Eur J Surg Oncol 2014;40(7):843–849.
50. Kitai T, Inomoto T, Miwa M, Shikayama T. Fluorescence navigation with indocyanine green for detecting sentinel lymph nodes in breast cancer. Breast Cancer 2005;12(3):211–215.
51. Fujisawa Y, Nakamura Y, Kawachi Y, Otsuka F. Indocyanine green fluorescence-navigated sentinel node biopsy showed higher sensitivity than the radioisotope or blue dye method, which may help to reduce false-negative cases in skin cancer. J Surg Oncol 2012;106(1):41–45.
52. Zaidi N, Bucak E, Okoh A, Yazici P, Yigitbas H, Berber E. The utility of indocyanine green near infrared fluorescent imaging in the identification of parathyroid glands during surgery for primary hyperparathyroidism. J Surg Oncol 2016;113(7):771–774.
53. Murawa D, Hirche C, Dresel S, Hünerbein M. Sentinel lymph node biopsy in breast cancer guided by indocyanine green fluorescence. Br J Surg 2009;96(11):1289–1294.
54. Tagaya N, Yamazaki R, Nakagawa A, et al. Intraoperative identification of sentinel lymph nodes by near-infrared fluorescence imaging in patients with breast cancer. Am J Surg 2008;195(6):850–853.
55. Voskuil FJ, Steinkamp PJ, Zhao T, et al; SHINE study group. Exploiting metabolic acidosis in solid cancers using a tumor-agnostic pH-activatable nanoprobe for fluorescence-guided surgery. Nat Commun 2020;11(1):3257.
56. Steinkamp P, Voskuil F, van der Vegt B, et al. Metabolic Acidosis in Cancer: A New Strategy Using a Ph Activated Imaging Agent for Fluorescence-Guided Surgery in Humans. Eur J Surg Oncol 2020;46(2):e163–e164.
57. Wang C, Wang Z, Zhao T, et al. Optical molecular imaging for tumor detection and image-guided surgery. Biomaterials 2018;157:62–75.
58. Wu J, Yuan Y, Tao XF. Targeted molecular imaging of head and neck squamous cell carcinoma: a window into precision medicine. Chin Med J (Engl) 2020;133(11):1325–1336.
59. Chen K, Chen X. Design and development of molecular imaging probes. Curr Top Med Chem 2010;10(12):1227–1236.
60. Barth CW, Gibbs SL. Fluorescence Image-Guided Surgery - a Perspective on Contrast Agent Development. In: Proc SPIE Int Soc Opt Eng 2020;11222.
61. Povoski SP, Neff RL, Mojzisik CM, et al. A comprehensive overview of radioguided surgery using gamma detection probe technology. World J Surg Oncol 2009;7(1):11.
62. Gioux S, Choi HS, Frangioni JV. Image-guided surgery using invisible near-infrared light: fundamentals of clinical translation. Mol Imaging 2010;9(5):237–255.
63. van Keulen S, Nishio N, Fakurnejad S, et al. The clinical application of fluorescence-guided surgery in head and neck cancer. J Nucl Med 2019;60(6):758–763.
64. Rosenthal EL, Warram JM, de Boer E, et al. Safety and tumor specificity of cetuximab-IRDye800 for surgical navigation in head and neck cancer. Clin Cancer Res 2015;21(16):3658–3666.
65. Voskuil FJ, de Jongh SJ, Hooghiemstra WTR, et al. Fluorescence-guided imaging for resection margin evaluation in head and neck cancer patients using cetuximab-800CW: A quantitative dose-escalation study. Theranostics 2020;10(9):3994–4005.
66. Nishio N, van den Berg NS, van Keulen S, et al. Optical molecular imaging can differentiate metastatic from benign lymph nodes in head and neck cancer. Nat Commun 2019;10(1):5044.
67. Vonk J, de Wit JG, Voskuil FJ, et al. Epidermal Growth Factor Receptor-Targeted Fluorescence Molecular Imaging for Postoperative Lymph Node Assessment in Patients with Oral Cancer. J Nucl Med 2022;63(5):672–678.
68. Rosenthal EL, Moore LS, Tipirneni K, et al. Sensitivity and specificity of cetuximab-IRDye800CW to identify regional metastatic disease in head and neck cancer. Clin Cancer Res 2017;23(16):4744–4752.
69. Demétrio de Souza França P, Kossatz S, Brand C, et al. A phase I study of a PARP1-targeted topical fluorophore for the detection of oral cancer. Eur J Nucl Med Mol Imaging 2021;48(11):3618–3630.
70. Gao RW, Teraphongphom N, de Boer E, et al. Safety of panitumumab-IRDye800CW and cetuximab-IRDye800CW for fluorescence-guided surgical navigation in head and neck cancers. Theranostics 2018;8(9):2488–2495.
71. van Keulen S, van den Berg NS, Nishio N, et al. Rapid, non-invasive fluorescence margin assessment: Optical specimen mapping in oral squamous cell carcinoma. Oral Oncol 2019;88:58–65.
72. van Keulen S, Nishio N, Birkeland A, et al. The Sentinel Margin: Intraoperative Ex Vivo Specimen Mapping Using Relative Fluorescence Intensity. Clin Cancer Res 2019;25(15):4656–4662.
73. Fakurnejad S, Krishnan G, van Keulen S, et al. Intraoperative Molecular Imaging for ex vivo Assessment of Peripheral Margins in Oral Squamous Cell Carcinoma. Front Oncol 2020;9:1476.
74. Koller M, Qiu SQ, Linssen MD, et al. Implementation and benchmarking of a novel analytical framework to clinically evaluate tumor-specific fluorescent tracers. Nat Commun 2018;9(1):3739.
75. de Jongh SJ, Tjalma JJJ, Koller M, et al. Back-Table Fluorescence-Guided Imaging for Circumferential Resection Margin Evaluation Using Bevacizumab-800CW in Patients with Locally Advanced Rectal Cancer. J Nucl Med 2020;61(5):655–661.
76. de Wit JG, Vonk J, Voskuil FJ, et al. EGFR-targeted fluorescence molecular imaging for intraoperative margin assessment in oral cancer patients: a phase II trial. Nat Commun 2023;14(1):4952.
77. Handgraaf HJM, Boonstra MC, Prevoo HAJM, et al. Real-time near-infrared fluorescence imaging using cRGD-ZW800-1 for intraoperative visualization of multiple cancer types. Oncotarget 2017;8(13):21054–21066.
78. Barrera JE, Miller ME, Said S, Jafek BW, Campana JP, Shroyer KR. Detection of occult cervical micrometastases in patients with head and neck squamous cell cancer. Laryngoscope 2003;113(5):892–896.
79. Wreesmann VB, Katabi N, Palmer FL, et al. Influence of extracapsular nodal spread extent on prognosis of oral squamous cell carcinoma. Head Neck 2016;38(Suppl 1):E1192–E1199.
80. den Toom IJ, Boeve K, Lobeek D, et al. Elective neck dissection or sentinel lymph node biopsy in early stage oral cavity cancer patients: The dutch experience. Cancers (Basel) 2020;12(7):1783.
81. Chen SL, Iddings DM, Scheri RP, Bilchik AJ. Lymphatic mapping and sentinel node analysis: current concepts and applications. CA Cancer J Clin 2006;56(5):292–309; quiz 316–317.
82. Zanoni DK, Stambuk HE, Madajewski B, et al. Use of Ultrasmall Core-Shell Fluorescent Silica Nanoparticles for Image-Guided Sentinel Lymph Node Biopsy in Head and Neck Melanoma: A Nonrandomized Clinical Trial. JAMA Netw Open 2021;4(3):e211936.
83. Wu VF, Malloy KM. Sentinel Node Biopsy for Head and Neck Cutaneous Melanoma. Otolaryngol Clin North Am 2021;54(2):281–294.
84. Lu G, Fakurnejad S, Martin BA, et al. Predicting Therapeutic Antibody Delivery into Human Head and Neck Cancers. Clin Cancer Res 2020;26(11):2582–2594.
85. Tummers WS, Warram JM, van den Berg NS, et al. Recommendations for reporting on emerging optical imaging agents to promote clinical approval. Theranostics 2018;8(19):5336–5347.
86. Chang AJ, De Silva RA, Lapi SE. Development and characterization of 89Zr-labeled panitumumab for immuno-positron emission tomographic imaging of the epidermal growth factor receptor. Mol Imaging 2013;12(1):17–27.

87. Walsh EM, Cole D, Tipirneni KE, et al. Fluorescence Imaging of Nerves During Surgery. Ann Surg 2019;270(1):69–76.
88. Bou-Samra P, Muhammad N, Chang A, et al. Intraoperative molecular imaging: 3rd biennial clinical trials update. J Biomed Opt 2023;28(5):050901.
89. Nishio N, van den Berg NS, Martin BA, et al. Photoacoustic Molecular Imaging for the Identification of Lymph Node Metastasis in Head and Neck Cancer Using an Anti-EGFR Antibody-Dye Conjugate. J Nucl Med 2021;62(5):648–655.
90. Pal R, Hom ME, van den Berg NS, et al. First Clinical Results of Fluorescence Lifetime-enhanced Tumor Imaging Using Receptor-targeted Fluorescent Probes. Clin Cancer Res 2022;28(11):2373–2384.
91. Rahim MK, Okholm TLH, Jones KB, et al. Dynamic CD8+ T cell responses to cancer immunotherapy in human regional lymph nodes are disrupted in metastatic lymph nodes. Cell 2023;186(6):1127–1143.e18.